Int. J. Heat Mass Transfer. Vol. 21, pp. 1403–1409
Pergamon Press Ltd. 1978. Printed in Great Britain

PREDICTION OF SKIN-FRICTION AND HEAT TRANSFER FROM COMPRESSIBLE TURBULENT BOUNDARY LAYERS IN ROCKET NOZZLES

K. MASTANAIAH*
ISRO Satellite Centre, Bangalore, India

(*Received* 9 *August* 1977 *and in revised form* 9 *January* 1978)

Abstract—An approximate method is reported for the rapid calculation of skin friction and heat transfer from compressible turbulent boundary layers in a convergent–divergent nozzle. The procedure is based on the use of Van Driest's eddy diffusivity model for the velocity profile, and the simultaneous solution of the integral form of momentum and total enthalpy equations. Generalisation of Crocco's integral in terms of a quadratic profile is suggested for the relation between total enthalpy and velocity in an accelerating boundary layer with heat transfer and non-unity Prandtl number. The numerical results using the proposed theory compare well with available data from heated air experiments in 10°–10° and 30°–15° convergent–divergent nozzles, and N_2H_4–N_2O_4 rocket nozzle with a 15° half-angle of divergence. The simplicity, reasonable accuracy and flexibility of the approach make it quite useful for predicting the thermal performance of rocket nozzles.

NOMENCLATURE

A_0,	constant = 26;
C_f,	friction coefficient, $C_f/2 = \tau_w/\rho_e u_e^2$;
C_p,	specific heat at constant pressure;
D,	damping function;
h,	static enthalpy;
I,	total enthalpy;
K_m,	mixing length constant = 0.4;
K,	acceleration parameter, $\frac{v_e}{u_e^2}\cdot\frac{\mathrm{d}u_e}{\mathrm{d}x}$;
k,	thermal conductivity;
k_T,	turbulent conductivity $= k+\rho C_p \varepsilon_H$;
M,	Mach number;
Pr,	Prandtl number evaluated at the wall;
P^+,	pressure gradient parameter, $-\frac{\mathrm{d}p}{\mathrm{d}x}\cdot\frac{v_e}{\rho_e u_\tau^3}$;
q,	heat flux;
r,	nozzle radius;
St,	Stanton number, $\frac{q_w}{(I_{aw}-I_w)\rho_e u_e}$;
u,	velocity component parallel to wall;
u^+,	dimensionless velocity, u/u_τ;
u_τ,	friction velocity, $(\tau_w/\rho_w)^{1/2}$;
v,	velocity component normal to wall;
x,	distance along wall;
y,	distance normal to wall;
y^+,	dimensionless normal distance, $\frac{\rho_w u_\tau y}{\mu_w}$;
z,	axial distance from throat.

Greek symbols

ε_H,	eddy diffusivity for heat;
δ^*,	displacement thickness $\simeq \int_0^\infty \left(1-\frac{\rho u}{\rho_e u_e}\right)\mathrm{d}y$;
ΔI,	(I_0-I_w);
θ,	momentum thickness $\simeq \int_0^\infty \frac{\rho u}{\rho_e u_e}\left(1-\frac{u}{u_e}\right)\mathrm{d}y$;
ρ,	density;
τ,	shear stress;
ϕ,	dimensionless velocity $= u/u_e$;
ψ,	energy thickness $\simeq \int_0^\infty \frac{\rho u}{\rho_e u_e}\left(1-\frac{I-I_w}{I_e-I_w}\right)\mathrm{d}y$.

Subscripts

aw,	adiabatic wall;
e,	free stream;
0,	stagnation;
w,	wall.

1. INTRODUCTION

THE DETERMINATION of temperature distribution in rocket nozzle walls subjected to high temperature and high heat flux environment requires the knowledge of total heat transferred from the combustion gases. The dominant mode of energy transport in chemical rocket engines is by convection, while the contribution due to thermal radiation is only about 10–20% of the total heat transferred. It is therefore important to accurately predict the convective heat transfer to the wall for achieving an optimum thermal protection system. Furthermore, new trends

*Presently graduate student, Department of Energy Engineering, University of Illinois at Chicago Circle, Chicago, IL 60680, U.S.A.

in smaller engines for upper stages and for spacecraft have also increased the demand for a detailed knowledge of friction losses and boundary-layer growth in the supersonic part of large expansion ratio nozzles in order to assess performance gains.

Many present day rocket engines operate under high pressure level, and consequently their throat Reynolds numbers are sufficiently large to ensure turbulent boundary-layer regime along the nozzle wall. An excellent review of the turbulent boundary-layer heat transfer in convergent–divergent nozzles has been given by Bartz [1]. Owing to the nature and complexity of the transfer process, many calculation procedures reported are essentially empirical.

A simple approximate closed-form solution for the local heat transfer coefficient has first been suggested by Bartz [2] in terms of a pipe flow correlation with a correction factor to accommodate the effects of compressibility, throat curvature and variation of transport properties across the boundary layer. Elliot, Bartz and Silver [3] have later reported a calculation method in which the energy and momentum integral equations are solved simultaneously, assuming the existence of similarity in the velocity and total temperature profiles of 1/7 power law with respect to their individual thicknesses that are related by an interaction parameter. Semi-empirical analyses are considered by Back and Cuffel [4] for describing heat transfer via the energy integral equation in conjunction with the measurements. Boldman *et al.* [5] have presented an empirical modification of [3] for estimating local heat transfer in converging–diverging nozzles. Their method involves the use of a modified Von Karman analogy which includes an acceleration term comprising the nozzle geometry and free stream velocity. Extensive nozzle data have, however, confirmed the general inadequacy of these empirical correlations, and limit their usefulness only for preliminary design requirements.

On the other hand, as the knowledge of the turbulent motion has increased, rigorous finite difference solution of the boundary-layer equations is carried out in their partial differential form along with higher order transport-equation models of turbulence. The popular solution methods are those of Patankar and Spalding [6] and Cebecci and Smith [7]. However, the differential methods often require excessive computing time, particularly in rocket motor applications involving the conjugate problem of transient heat conduction, and may not always justify their regular use for thermal design purposes.

From the foregoing considerations, the present paper aims to present a solution capable of meeting the demands of acceptable accuracy, lower execution times and enough flexibility for incorporating, to the extent possible, the knowledge gained in the structure of turbulent boundary layer. Attention is focussed primarily on the development of an appropriate revision of the Crocco integral for the total enthalpy–velocity profiles in compressible turbulent boundary layers under pressure gradient and heat transfer.

2. ANALYSIS

For a compressible turbulent boundary layer in axisymmetric flow with pressure gradient, Von Karman's form of integral equations for momentum and energy can be written as follows:

Momentum:

$$\frac{\mathrm{d}\theta}{\mathrm{d}x}+\theta\left[\left(2+\frac{\delta^*}{\theta}-M_e^2\right)\frac{1}{u_e}\frac{\mathrm{d}u_e}{\mathrm{d}x}+\frac{1}{r}\frac{\mathrm{d}r}{\mathrm{d}x}\right]=\frac{C_f}{2}. \quad (1)$$

Energy:

$$\frac{\mathrm{d}\psi}{\mathrm{d}x}+\psi\frac{\mathrm{d}}{\mathrm{d}x}[\ln(\rho_e u_e \Delta I r)]=\frac{St}{2}\frac{(I_{aw}-I_w)}{\Delta I}. \quad (2)$$

Constant average specific heat and one-dimensional core flow are assumed in the analysis.

(a) *Velocity profiles*

In order to solve for the velocity boundary layer, we assume that the shear stress is constant across the boundary layer and that Van Driest's eddy diffusivity model is applicable throughout, in which a damping function is introduced for the law of the wall region based on Prandtl's mixing length concept. Cebecci's extension [7] of Van Driest model is incorporated to take into account the effect of pressure gradient.

Under the assumptions made here, the velocity distribution in dimensionless wall variables can be written was:

$$\frac{\mathrm{d}y^+}{\mathrm{d}u^+}=\frac{1}{2}\left\{\frac{\mu}{\mu_w}+\left[\left(\frac{\mu}{\mu_w}\right)^2+4\frac{\rho}{\rho_w}K_m^2(y^+)^2D^2\right]^{1/2}\right\} \quad (3)$$

where

$$D=1-\exp(-y^+/A^+) \quad (4)$$

$$A^+=A_0^+(1-11.8P^+). \quad (5)$$

(b) *Total enthalpy–velocity relation*

It is generally convenient to establish a satisfactory relationship between the total enthalpy and velocity in the boundary layer so that the need for a separate solution of the thermal boundary layer is obviated. In flow situations typical of rocket nozzles, where the effects of strong favourable pressure gradients, heat transfer and non-unity Prandtl number are manifest, the total enthalpy–velocity relation does not obey the well-known Crocco integral

$$I^*=\phi. \quad (6)$$

An appropriate extension of the Crocco relation will therefore be developed along the lines of Tetervin [8] for application in the nozzle heat-transfer problem. Since the viscous effects in the laminar sublayer of an accelerating turbulent boundary layer are important for inferring the transport quantities [9], we place emphasis on the wall region in which is assumed a quadratic enthalpy–velocity profile of the form

$$I^* = A_1\phi + A_2\phi^2. \tag{7}$$

The parameters A_1 and A_2 are obtained from the boundary conditions at the wall. From the definition of heat flux in compressible flow, we have

$$-q = u\tau + k_T\frac{\partial T}{\partial y}. \tag{8}$$

With the notation $\phi = u/u_e$, $f = \tau/\tau_w$ and $g = q/q_w$, equation (8) yields

$$\frac{u_e^2}{2}\phi f + \frac{u_e}{2}\frac{k_T}{C_p}\frac{f}{\tau}\frac{\partial h}{\partial y} = -\frac{q_w g}{\rho_e u_e C_f}. \tag{9}$$

From equations (7) and (8), it can be shown that

$$A_1 = 2\frac{St}{C_f}Pr\frac{(I_{aw}-I_w)}{(I_0-I_w)} \tag{10}$$

which represents a modified Reynolds-analogy factor.

To obtain A_2, we now differentiate equation (9) with respect to y and obtain the relation

$$\frac{u_e^2}{2}\left[\phi\frac{\partial f}{\partial y} + f\frac{\partial \phi}{\partial y}\right] + \frac{u_e}{2}\frac{k_T}{\tau_w C_p}\frac{\partial^2 h}{\partial y^2} = -\frac{q_w}{\rho_e u_e C_f}\frac{\partial g}{\partial y}. \tag{11}$$

The differential boundary-layer equation for total enthalpy is now invoked, and is given by

$$\rho u\frac{\partial I}{\partial x} + (\rho v + \overline{\rho' v'})\frac{\partial I}{\partial y} = -\frac{\partial q}{\partial y}. \tag{12}$$

Equations (7), (11) and (12) applied at the wall result in an expression for A_2 as

$$A_2 = \frac{(1-Pr)}{\Delta I}\frac{u_e^2}{2} + \frac{h_w}{h_0}\frac{\mu_w \rho_w}{\rho_e^2 u_e}\cdot\frac{2A_1}{C_f^2}\frac{\mathrm{d}(\ln M_e)}{\mathrm{d}x}. \tag{13}$$

In view of the uncertainty of the boundary conditions in the outer part of the velocity and thermal boundary layers, we assume that equation (7) is applicable for the turbulent portion of the boundary layer also. However, the error due to this assumption does not significantly effect the evaluation of the boundary-layer integrals, which are rather insensitive to the accuracy with which the friction and heat transfer are determined. Equation (7) will reduce to the Crocco profile in the appropriate limit.

It may be noted that the expressions for A_1 and A_2 given above are consistent with those given recently by Rasmussen [10], who has proposed a cubic profile for the enthalpy with the outer boundary condition $I^* = 1$ at $\phi = 1$. In that reference, the temperature and velocity profiles are in transformed variables, and no comparisons are made between the predicted and measured enthalpy–velocity values in physical co-ordinates.

In the course of the present investigation, Rasmussen's cubic profile has been found to be inadequate when compared to the available experimental data, since the measured enthalpy values lie considerably higher than the predictions in the sublayer, resulting in unacceptable estimates for heat-transfer rates. The inclusion of the cubic term and the associated outer boundary condition are believed to be responsible for the apparent inadequacy of his profile. On the other hand, the quadratic profile proposed in the present paper has offered satisfactory agreement between the theory and experiment, which the comparisons will illustrate later in the text.

3. SOLUTION PROCEDURE

Equations (1) and (2) constitute a system of two coupled ordinary differential equations. The numerical solution starts with known or presumed values of the quantities θ, ψ, δ^*, $C_f/2$ and St at the initial station near the nozzle entrance. Using $C_f/2$ and St at the ith station along the nozzle, the velocity profile $u^+ - y^+$ is solved for the $i+1$ station by second order Runge–Kutta library subroutine RK2. The boundary-layer integral parameters δ^*, θ and ψ are then computed by integration using Simpson's rule. Based on this information, new values of $C_f/2$ and St are now generated by a simultaneous solution of the integral equations (1) and (2). The iteration at the $i+1$ station is continued until convergence in St and $C_f/2$ is attained within the desired accuracy. The calculations are performed on an IBM-360/44 digital computer.

4. COMPARISON WITH EXPERIMENTAL DATA

The validity of the proposed quadratic enthalpy–velocity profile has been tested by comparing the computed results with existing boundary-layer data from heated air experiments in convergent–divergent nozzles [4, 11], heat flux measurements in N_2O_4–N_2H_4 liquid propellant rocket nozzle [12], and boundary-layer data on air flowing over an adiabatic flat plate [13] with zero pressure gradient.

(a) *Heated air data of Back and Cuffel* [4]

In [4, 9] by Back and Cuffel, turbulent boundary-layer and heat-transfer measurements are made in a cooled convergent–divergent nozzle with a half angle of 10° and with 10:1 contraction ratio. In their experiments, $p_0 = 10.35$ bar, $T_0 = 835$ K and $T_w/T_0 \simeq 0.5$ are considered. The temperature is chosen such that radiation is negligible. Air is the working fluid with $Pr = 0.7$. The nozzle throat diameter, inlet length and total length are 40.39 mm, 127 mm and 526 mm respectively. The operating conditions are such that the boundary layer remains essentially turbulent. The controlled measurements provide information on turbulent boundary layers subject to the kind of flow acceleration found in practice, and in this regard the nozzle shape resembles a rocket

Table 1. Comparison of predictions with experimental data for boundary-layer thickness parameters, skin-friction and heat transfer

Station No.	$\frac{\rho_e u_e \theta}{\mu_e}$	M_e	z, m	δ^*, mm Pred.	δ^*, mm Expt.	θ, mm Pred.	θ, mm Expt.	ψ, mm Pred.	ψ, mm Expt.	$C_f/2 \times 10^3$ Pred.	$C_f/2 \times 10^3$ Expt.	$St \times 10^3$ Pred.	$St \times 10^3$ Expt.
1	9600	0.072	−0.2225		0.705		2.01		2.77		2.5		1.75
2	8300	0.104	−0.1655	0.0716	−0.0717	1.195	1.195	2.44	2.54	1.91	2.66	2.23	1.84
3	8100	0.137	−0.127	−0.182	−0.303	0.858	0.89	2.276	2.42	1.95	2.4	2.177	1.775
4	9600	0.194	−0.089	−0.262	−0.213	0.624	0.76	1.819	2.03	1.95	2.3	2.093	1.75
5	12800	3.57	+0.212		−0.308	1.061	0.965	3.372	3.00	0.96	0.88	0.734	0.634

thrust chamber. The heat-transfer measurements are mentioned to be accurate to about $\pm 5\%$ and boundary-layer thickness to within 10–20%.

In the calculations, data at station 1 is taken to be the initial condition. An interval of $\Delta x = 0.02$ m is employed. The execution time for one run through the nozzle is only about 1.5 min.

Table 1 compares the predictions from the present theory with the observed data for the boundary-layer, skin-friction and heat-transfer parameters at five stations along the nozzle. It is seen that the calculated values for δ^*, θ and ψ are in good agreement with the measurements. In the convergent for stations 1 to 4 with $M_e \leqslant 0.194$, the predicted $C_f/2$ and St lie respectively 15–30% below and 20–23% above the data. At station 5 in the far divergent for which $M_e = 3.57$, $C_f/2$ is predicted within 9% and St within 16% of the measured values. At the throat, where maximum heat flux occurs, the predicted Stanton number is about 20% higher than the experimental value.

Figures 1(a) and (b) depict the comparison of predicted total enthalpy–velocity profiles with the experimental values. The Crocco line and the predictions using Rasmussen's cubic profile are also represented in the figures. From Fig. 1(a), it is seen that in the convergent at $M_e = 0.194$, the present theory is compared with the experiment in the range $0.55 < \phi < 1$ for which data exist, and yields enthalpy values which are somewhat above the data except near the edge of the boundary layer. The cubic profile, however, appears to be inconsistent with the measurements.

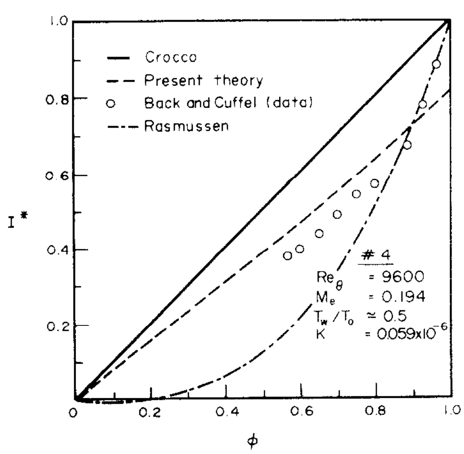

FIG. 1(a). Comparison of total enthalpy–velocity profiles in 10°–10° nozzle convergent.

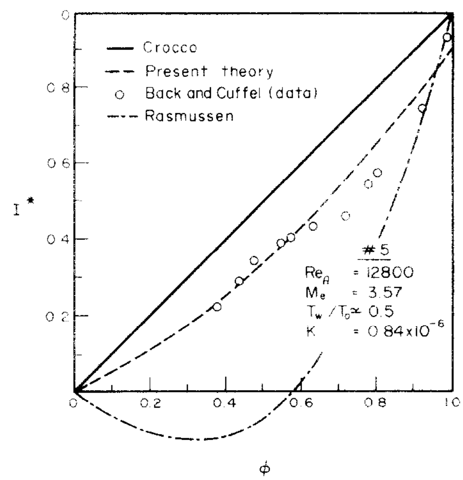

FIG. 1(b). Comparison of total enthalpy–velocity profiles in 10°–10° nozzle divergent.

Figure 1(b) suggests that in the divergent where $M_e = 3.57$, the agreement between the present theory and the data is very good in the range $0.4 < \phi < 0.6$, which includes part of the viscous sublayer. The enthalpy values using Rasmussen's cubic profile fall considerably below the measurements as the wall is approached, and yield inadmissible value for the Stanton number. Note that in both the cases, Crocco profile departs significantly from the data and lies above the measured enthalpy values.

Figures 1(a) and (b) also reveal that the present theory yields values of $I^* < 1$ at $\phi = 1$, thus indicating that in turbulent flow under modest acceleration, the thermal boundary layer may penetrate beyond the edge of the velocity boundary layer leading to a thermal superlayer effect [14] which contributes in part to the decrease in Stanton number. The experimental detection of the extent of the thermal superlayer is indeed difficult because of its small magnitude as mentioned by Launder [14], and also due to the uncertainty in determining the edge of the boundary layer. The inadequacy of Rasmussen's cubic profile is perhaps due to the fact that in an accelerating flow, the assumption that the

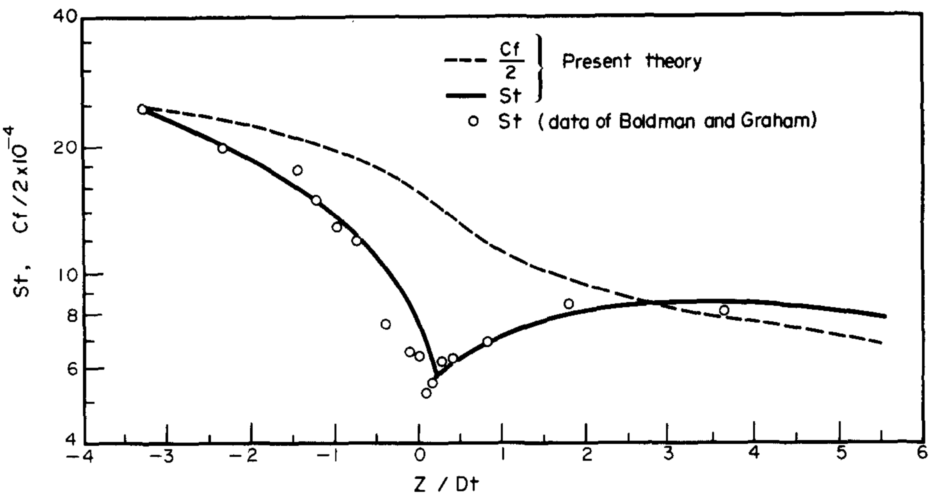

FIG. 2. Distribution of Stanton number and skin-friction coefficient along 30°–15° converging–diverging nozzle.

thermal and velocity boundary layers coincide becomes invalid.

(b) *Heated air data of Boldman and Graham* [5]

Boldman and Graham [5] have obtained boundary-layer and heat-transfer measurements in a 30°–15° nozzle, which is a more practical configuration. Air is the working medium with $p_0 = 20.7$ bar, $T_0 = 539$ K and $T_w/T_0 \simeq 0.8$. The nozzle throat diameter, contraction ratio, convergent length and total nozzle length are 37.9 mm, 18.98 mm, 120 mm and 409 mm respectively.

In the calculations, initial values of δ^*, θ and ψ are taken as 1.5 mm, 1.6 mm and 1.43 mm respectively which are obtained from the measurements at the entrance. An interval Δx of 0.02 m is employed. The initial value of $C_f/2$ is assumed to be equal to the measured Stanton number based on free stream density.

Figure 2 displays the calculated St and $C_f/2$ distributions along the nozzle. The Stanton number data are shown for comparison purposes. The original Stanton number data of [5] are based on the density corresponding to Eckert reference temperature, and are converted to free stream values. Skin friction data are not, however, available for comparison with the present theory. Examination of Fig. 3 suggests that the trend of predicted Stanton number using the proposed theory is in fair agreement with the measured data. At the throat, the calculated St lies 20% above the experimental value and appears to be satisfactory for engineering design. It can be seen that there is a marked decrease in Stanton number as the throat is approached with a minimum occurring shortly beyond the throat, and a subsequent recovery in the divergent portion. There is, however, no such marked decrease in $C_f/2$ along the nozzle. The significant reduction in heat transfer near the throat is attributed to the high value of the acceleration parameter, K, which is about 2×10^{-6} near the nozzle entrance. Because of this high acceleration, the turbulent boundary layer becomes laminar-like near the wall, presumably due to the loss of turbulent transport in the wall vicinity, and the process is known as laminarization. Beyond the throat, where acceleration is relatively small, there is a forward transition from near-laminar to fully turbulent flow. This phenomena has been extensively studied by many investigators both in incompressible and compressible flows, see for example [15–17].

The total enthalpy–velocity profiles are depicted in Fig. 3 at the far divergent with $M_e = 4.4$. It is evident that the present theory using the quadratic profile for $I^* - \phi$ compares well with the experimental data in the range $0.5 < \phi < 1$, thus demonstrating the soundness of the proposed expression. Calculations have also indicated that the cubic profile due to Rasmussen again results in wild values for the enthalpy profile such as found in Fig. 1, and are not however presented here.

(c) *Liquid rocket nozzle data of Welsh and Witte* [12]

Since the primary aim of this investigation is to

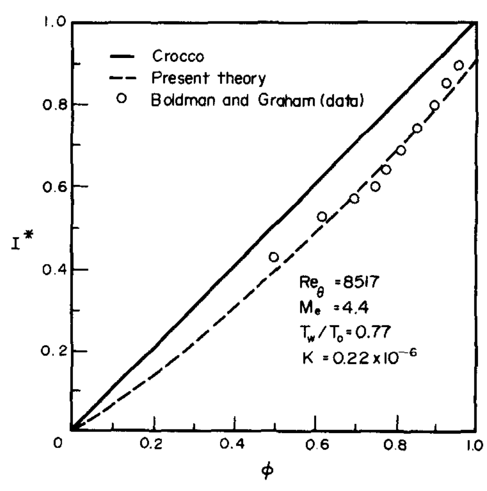

FIG. 3. Comparison of total enthalpy–velocity profiles in 30°–15° nozzle divergent.

predict heat transfer in rocket nozzle, it is imperative that the validity of the improved theory is examined by comparing the calculated results with observed data on rocket nozzles, which are characterised by high stagnation temperatures. Unfortunately, to the author's knowledge, there appears to be little data on detailed boundary-layer surveys in practical rocket nozzles because of the difficulty of measurements. The only means of comparison is the measured wall heat flux integrated circumferentially over small segments.

The data of Welsh and Witte [12] is considered for comparison purposes. They have obtained heat flux data on N_2O_4–N_2H_4 rocket nozzle with 4:1 contraction ratio. The characteristic velocity is 1540 m/s. The propellant mixture ratio and the characteristic length, L^*, of the combustion chamber are 1.01 and 0.6 m respectively. The combustion temperature $T_0 \simeq 2580$ K and stagnation pressure $p_0 = 9.93$ bar. The specific heat ratio is 1.22. Wall to total temperature ratio of 0.19 is considered. The nozzle divergent half-angle is 15°, and the throat diameter is 0.635 m.

The calculation starts at 0.04 m upstream throat with an assumed value of 1.5 mm for δ^*, θ and ψ, and a value of 0.0025 for $C_f/2$ and St. An interval Δx of 0.01 m is considered.

Figure 3 shows the comparison of the present predictions with the experimental heat flux distribution along the nozzle. Also shown in the figure is the calculated heat flux using the standard Bartz equation [2]. It is interesting to note that the present theory is in excellent agreement with the measured heat flux data along the nozzle including the throat region. The results from the Bartz equation, however, lie above the experimental data resulting in about 6% overestimation of the heat flux at the throat. The departure of the Bartz equation from the data increases along the downstream, and is about 35% above the measured heat flux in the far divergent, 0.082 m away from the throat.

It may however be noted that the present solution assumes negligible influence of other factors like injection effects, combustion chamber oscillations, free stream turbulence, and chemical reactions within the boundary layer on the net wall heat flux.

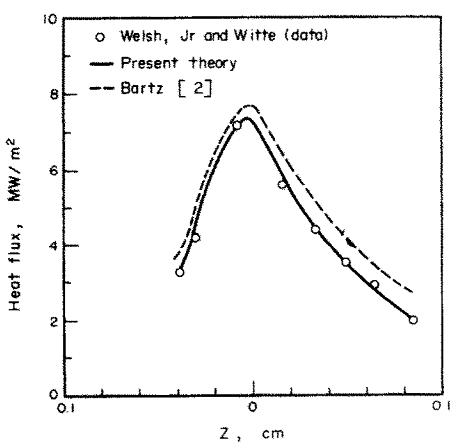

FIG. 4. Comparison of heat flux in N_2O_4–N_2H_4 liquid rocket nozzle.

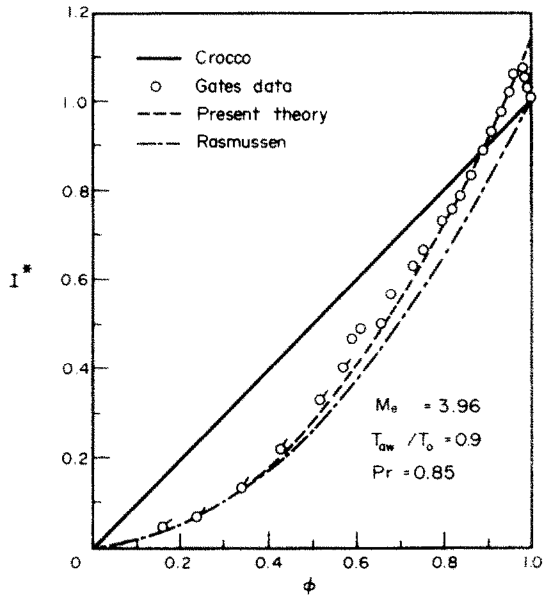

FIG. 5. Comparison of total enthalpy–velocity profiles for adiabatic flat plate with zero pressure gradient.

(d) *Data on adiabatic flat plate* [13]

As a further test to the validity of the proposed profile, the calculated enthalpy–velocity profile is compared under a limiting case with air data by Gates [13] in compressible flow over an adiabatic flat plate with zero pressure gradient at $M_e = 3.96$, $T_{aw}/T_0 = 0.9$ and $Pr = 0.85$. Figure 4 illustrates these comparisons. Rasmussen's profile is also indicated in the figure. The flagged symbols represent the extrapolated data as given in [13]. It is seen that the quadratic profile is able to predict the overshoot of total temperature near the edge of the boundary layer, which is characteristic of adiabatic flows with non-unity Prandtl number as indicated by Van Driest's analysis [18]. The agreement between the present predictions and the data is quite good, while Rasmussen's profile lies below the data throughout the boundary layer and is unable to predict the total enthalpy overshoot, obviously due to the boundary condition $I^* = 1$ at $\phi = 1$. This example therefore serves to further substantiate the generality of the present profile.

5. CONCLUDING REMARKS

A quadratic profile for the total-enthalpy as a function of velocity has been proposed for compressible turbulent boundary layers with pressure gradient, heat transfer and non-unity Prandtl number, and is found to agree satisfactorily with the existing data on convergent–divergent nozzles, and adiabatic flows over a flat plate with zero pressure gradient. The inadequacy of the cubic profile advanced earlier by Rasmussen has been demonstrated. Using the present profile, a simple and rapid calculation procedure has been suggested for successfully predicting skin-friction and heat transfer in rocket nozzles. It is believed that the simplicity and elegance of the improved expression for the total enthalpy will have considerable practical utility in a variety of flow geometries involving compressible as well as incompressible flows.

Acknowledgements—The author expresses his gratitude to the referee for his constructive criticism and to the editor Prof. D. B. Spalding for his helpful suggestion and encouragement. Thanks are also due to his colleagues Dr. T. G. K. Murthy, Mr. K. C. Navada and Mr. S. Hussain Sahib for useful comments.

REFERENCES

1. D. R. Bartz, Turbulent boundary-layer heat transfer from rapidly accelerating flow of rocket combustion gases and of heated air, in *Advances in Heat Transfer*, edited by J. P. Hartnett and T. F. Irvine, Vol. 2, pp. 1–108. Academic Press, New York (1965).
2. D. R. Bartz, A simple equation for rapid estimation of rocket nozzle convective heat transfer coefficients, *Jet Propulsion* **27**, 49 (1957).
3. D. G. Elliott, D. R. Bartz and S. Silver, Calculation of turbulent boundary-layer growth and heat transfer in axisymmetric nozzles, TR 32-387, Jet Propulsion Laboratory, Pasadena, California (1963).
4. L. H. Back and R. F. Cuffel, Turbulent boundary layer and heat transfer measurements along a convergent–divergent nozzle, *J. Heat Transfer* **93**, 397 (1971).
5. D. R. Boldman, J. F. Schmidt and E. C. Robert, prediction of local and integrated heat transfer in nozzles using an integrated turbulent boundary layer method, NASA TND—6595 (1972).
6. S. V. Patankar and D. B. Spalding, *Heat and Mass Transfer in Boundary Layers*. Morgan-Grampian Press, London (1967).
7. T. Cebecci and A. M. O. Smith, *Analysis of Turbelent Boundary Layers*. Academic Press, New York (1974).
8. N. Tetervin, Approximate calculation of Reynolds analogy for turbulent boundary layer with pressure gradient, *AIAA Jl* **7**, 1079 (1969).
9. L. H. Back and R. F. Cuffel, Relationship between temperature and velocity profiles in a turbulent boundary layer along a supersonic nozzle with heat transfer, *AIAA Jl* **8**, 2066 (1970).
10. M. L. Rasmussen, on compressible turbulent boundary layers in the presence of favourable pressure gradients, ASME Paper No. 75-WA/HT-53 (1975).
11. D. R. Boldman and R. W. Graham, Heat Transfer and Boundary layer in conical nozzles, NASA TND-6594, February (1972).
12. W. E. Welsh, Jr., and A. B. Witte, A comparison of analytical and experimental local heat fluxes in liquid propellant thrust chambers, *J. Heat Transfer* **84**, 19 (1962).
13. D. L. Whitefield and M. D. High, Velocity–temperature relations in turbulent boundary layers in non-unity Prandtl numbers, *AIAA Jl* **15**, 425 (1977).
14. B. E. Launder and F. C. Lockwood, An aspect of heat transfer in accelerating turbulent boundary layers, *J. Heat Transfer* **91**, 229 (1969).
15. P. M. Moretti and W. M. Kays, Heat Transfer to a turbulent boundary layer with varying free-stream velocity and surface temperature—an experimental study, *Int. J. Heat Mass Transfer* **9**, 1187–1202 (1965).
16. L. H. Back, R. F. Cuffel and P. F. Massier, Laminarization of a turbulent boundary layer in nozzle flow—Boundary layer and heat transfer measurements with wall cooling, *J. Heat Transfer* **92**, 333 (1970).
17. E. Talmor and N. Weber, Heat transfer from boundary layers undergoing an acceleration induced reverse transition, *A.I.Ch.E. Jl* **16**, 446 (1970).
18. E. R. Van Driest, The turbulent boundary layer with variable Prandtl number, pp. 257–271. 50 Jahre Grenzschichtferschung Friedr. Vieweg Sohn, Braunschweig (1955).

PREDICTION DU FROTTEMENT PARIETAL ET DU TRANSFERT THERMIQUE POUR LES COUCHES LIMITES TURBULENTES ET COMPRESSIBLES DANS LES TUYERES DE FUSEE

Résumé—On décrit une méthode approchée pour le calcul rapide du frottement pariétal et du transfert thermique pour les couches limites turbulentes et compressibles dans une tuyère convergente–divergente. La procédure est basée sur l'utilisation du modèle de diffusivité turbulente donné par Van Driest pour le profil de vitesse et la solution simultanée des équations de quantité de mouvement et d'enthalpie totale. Une généralisation de l'intégrale de Crocco par un profil quadratique est suggérée pour la relation entre l'enthalpie totale et la vitesse dans une couche limite accélérée avec transfert thermique et nombre de Prandtl différent de l'unité. Les résultats numériques s'accordent bien avec les données disponibles d'expériences sur l'air chaud dans des tuyères convergentes—divergentes 10—10° et 35°—15° et sur une tuyère de fusée N_2 H_4—N_2 O_4 avec un demiangle de 15° au divergent. La simplicité, la précision raisonnable et la flexibilité de l'approche rendent celle-ci utile pour la prévision des performances thermiques des tuyères de fusée.

BERECHNUNG VON REIBUNGS–DRUCKABFALL UND WÄRMEÜBERGANG IN KOMPRESSIBLEN TURBULENTEN GRENZSCHICHTEN IN RAKETENDÜSEN

Zusammenfassung—Es wird über eine Näherungsmethode zur schnellen Berechnung von Reibungs–Druckabfall und Wärmeübergang in kompressiblen turbulenten Grenzschichten einer konvergent–divergenten Düse berichtet. Das Verfahren stützt sich auf das Modell des turbulenten Austausches nach van Driest für das Geschwindigkeitsprofil und auf die simultane Lösung der Integralform von Impuls– und Energiegleichung. Die Verallgemeinerung von Crocco's Integral, ausgedrückt durch ein quadratisches Profil, wird empfohlen für die Beziehung zwischen Gesamtenthalpie und Geschwindigkeit einer beschleunigten Grenzschicht mit Wärmeübergang und Prandtl–Zahlen, die größer als eins sind. Die numerischen Ergebnisse der vorgeschlagenen Theorie stimmen gut mit vorhandenen Meßwerten von Heißluft–Experimenten in konvergent–divergenten $+10°/-10°$–Düsen und $+35°/-15°$–Düsen sowie mit $N_2H_4-N_2O_4$–Raketendüsen mit einem halben Öffnungswinkel von 15° überein. Die Einfachheit, angemessene Genauigkeit und Flexibilität der Näherungsbeziehung lassen sie sehr brauchbar für die Berechnung des thermischen Verhaltens von Raketendüsen erscheinen.

РАСЧЁТ ПОВЕРХНОСТНОГО ТРЕНИЯ И ТЕПЛОПЕРЕНОСА В РАКЕТНЫХ СОПЛАХ В СЖИМАЕМЫХ ТУРБУЛЕНТНЫХ ПОГРАНИЧНЫХ СЛОЯХ

Аннотация — Предложен приближенный метод расчёта поверхностного трения и переноса тепла в сжимаемых турбулентных пограничных слоях в конфузорно-диффузорном сопле. Расчёт основан на использовании модели вихревой диффузии Ван-Дриста для профиля скорости и одновременном решении интегральных уравнений импульса и суммарной энтальпии. В соотношении между суммарной энтальпией и скоростью в ускоряющемся пограничном слое при наличии теплообмена и числе Прандтля, не равном единице, предложено использовать интеграл Крокко, выраженный через квадратичный профиль скорости. Полученные численные результаты хорошо согласуются с имеющимися экспериментальными данными для нагретого воздуха в конфузорно-диффузорных соплах с 10°–10° и 35°–15°, соответственно, и в N_2H_4–N_2O_4 ракетном сопле с 15° углом полураствора. Простота, достаточная точность и гибкость метода делают его вполне пригодным при расчётах теплового кпд ракетных сопел.